INTERNATIONAL JOURNAL FOR NUMERICAL METHODS IN FLUIDS, VOL. 5, 405–425 (1985)

APPLICATION OF THE DUFORT–FRANKEL AND SAUL'EV METHODS WITH TIME SPLITTING TO THE FORMULATION OF A THREE DIMENSIONAL HYDRODYNAMIC SEA MODEL

ALAN M. DAVIES

Institute of Oceanographic Sciences, Bidston Observatory, Birkenhead, Merseyside L43 7RA, England.

SUMMARY

A three dimensional hydrodynamic sea model of an arbitrary sea area is formulated using sigma co-ordinates in the vertical. The solution of the equations using finite difference grids in the horizontal and the vertical is described.

Discretization of the vertical viscosity term in the hydrodynamic equations using the DuFort–Frankel and Saul'ev methods is developed. Some numerical instabilities occur with the DuFort–Frankel method which can be overcome by splitting the hydrodynamic equations into equations describing the mean flow and equations describing the deviations from it. The computational advantages of solving these equations with different time steps are discussed.

The accuracy and stability of the various methods is demonstrated for wind induced flow in a simple rectangular basin having dimensions representing the North Sea.

KEY WORDS DuFort–Frankel Saul'ev Instability Sea Model Hydrodynamic Three-dimensional Time-splitting

1. INTRODUCTION

The explicit time integration method for the solution of the two dimensional and three dimensional hydrodynamic equations which describe motion in a sea area is used extensively in oceanographic problems, although implicit methods are becoming more popular.

In a two dimensional vertically integrated model the length of the time step used with the explicit method to integrate the hydrodynamic equations is in general governed by the speed of propagation of the free surface wave (the Courant–Friedrich–Lewy (C.F.L.) criterion). In a three dimensional model, if an explicit time integration method is used then besides the C.F.L. stability condition there is also a condition imposed by the vertical diffusion term which is related to the magnitude of the vertical eddy viscosity and the water depth. In many problems, particularly in the application of three dimensional models to flow in an estuary,[1,2] where the vertical viscosity can be high (of order 1000 cm^2/s) and the water depth in places is shallow (typically less than 5 m) then the magnitude of the time step used to integrate the hydrodynamic equations is determined by the stability condition associated with the vertical diffusion term. In many cases this forces the time step to be an order of magnitude less than that determined by the CFL criterion. Such a small time step can be particularly restrictive and require considerable computer time.

In order to overcome this problem, it is necessary to treat the diffusion term in a semi-implicit manner. By this method the stability condition imposed by the diffusion term is removed, although the equations can still be integrated forward through time using a simple time stepping algorithm.

0271–2091/85/050405–21$02.10

Received 5 March 1984
Revised 30 October 1984

In this paper the DuFort–Frankel[3] and the Saul'ev[4] difference methods are used to represent the vertical diffusion term. Both methods are known[5,6] to be unconditionally stable when applied to the solution of a one dimensional problem involving only the diffusion term. However in this paper we show that the application of the DuFort–Frankel method to the discretization of the vertical diffusion term in the three dimensional hydrodynamic equations describing flow in a sea area is not unconditionally stable. In fact the term in the hydrodynamic equations which involves the gradient of sea surface elevation influences the time step which can be used in the DuFort–Frankel method. The Saul'ev integration method however is not affected by the gradient term, and remains stable when used to integrate the diffusion term in the hydrodynamic equations.

A number of authors[1,2] have noted stability problems associated with the vertical diffusion term when the Dufort–Frankel method was used to discretize this term in the three dimensional hydrodynamic equations. These authors had to use a small time step in order to retain numerical stability.[2] Sengupta *et al.*[1] reported that their time step was restricted by the diffusion term.

In this paper we show that this problem can be overcome by integrating the equations involving the mean flow and sea surface elevation gradient, separately from the equations describing the current structure (internal flow). By this means the influence of the elevation gradient upon the time step used in the DuFort–Frankel method is removed. By using this splitting approach the equations describing the internal flow can be integrated using a much longer time step than that used for the mean flow (a time splitting method).

The time step used to integrate the external motion however is still restricted by the C.F.L. condition when explicit time integration is used. However, since a major part of the computation is involved in integrating the equations describing the internal flow, then a significant computational saving can be achieved by using as long a time step as possible to integrate these equations. Care has to be taken in the choice of this time step since the two sets of equations describing mean and internal flow are coupled through bottom friction and the non-linear terms. Consequently the time step for the internal flow cannot be too large if bottom friction is to be accurately reproduced in a rapidly evolving flow. (The time splitting algorithm developed here is analogous to that used by Davies[7] for solving the three dimensional hydrodynamic equations using the Galerkin method through the vertical).

In Section 2 of this paper the separation into internal and mean flows and the numerical solution using a sigma co-ordinate system[8–10] with grid boxes through the vertical is considered. Both the DuFort–Frankel and the Saul'ev methods are applied to the discretization of the diffusion term which occurs in the equation describing the internal flow and are found to be unconditionally stable when applied to the solution of this equation.

The effects of using various lengths of time step upon the accuracy of the solution are discussed in detail in this paper. The accuracy and stability of both the DuFort–Frankel and the Saul'ev methods are examined in Section 4, using an idealized linear model of the North Sea. A non-linear model is also considered.

2. HYDRODYNAMIC EQUATIONS AND SIGMA CO-ORDINATE TRANSFORMATION

2.1. *Hydrodynamic equations*

The non-linear hydrodynamic equations of continuity and motion, in Cartesian co-ordinates, are given by

$$\frac{\partial \zeta}{\partial t} + \frac{\partial}{\partial x}\int_{-\zeta}^{h} u\,dz + \frac{\partial}{\partial y}\int_{-\zeta}^{h} v\,dz = 0 \tag{1}$$

$$\frac{\partial u}{\partial t}+u\frac{\partial u}{\partial x}+v\frac{\partial u}{\partial y}+w\frac{\partial u}{\partial z}-\gamma v=-g\frac{\partial \zeta}{\partial x}+\frac{\partial}{\partial z}\left(N\frac{\partial u}{\partial z}\right) \tag{2}$$

$$\frac{\partial v}{\partial t}+u\frac{\partial v}{\partial x}+v\frac{\partial v}{\partial y}+w\frac{\partial v}{\partial z}+\gamma u=-g\frac{\partial \zeta}{\partial y}+\frac{\partial}{\partial z}\left(N\frac{\partial v}{\partial z}\right) \tag{3}$$

$$w(z)=\frac{\partial}{\partial x}\int_z^h u\,\mathrm{d}z+\frac{\partial}{\partial y}\int_z^h v\,\mathrm{d}z \tag{4}$$

where we denote by,

t	time,
x, y, z	a left handed set of Cartesian co-ordinates, with z the depth below the undisturbed surface
h	undisturbed depth of water
ζ	elevation above undisturbed depth
u, v, w	components of current at depth z in directions of increasing x, y, z, respectively
ρ	density of sea water
γ	geostrophic coefficient, taken as constant
g	acceleration due to gravity
N	coefficient of vertical eddy viscosity

The surface boundary conditions, evaluated at the free surface $z=-\zeta$, are given by

$$-\rho\left(N\frac{\partial u}{\partial z}\right)_{-\zeta}=F_s,\quad -\rho\left(N\frac{\partial v}{\partial z}\right)_{-\zeta}=G_s \tag{5}$$

with F_s, G_s the x, y components of the wind stress.

The sea-bed boundary conditions, evaluated at $z=h$ are given by

$$-\rho\left(N\frac{\partial u}{\partial z}\right)_{h}=F_B,\quad -\rho\left(N\frac{\partial v}{\partial z}\right)_{h}=G_B \tag{6}$$

with F_B, G_B the x, y components of bottom stress.

In a non-linear model, bottom stress is in general parametrized using a quadratic law of bottom friction, of the form

$$F_B=K\rho u_d(u_d^2+v_d^2)^{1/2},\quad G_B=K\rho v_d(u_d^2+v_d^2)^{1/2} \tag{7}$$

with K a coefficient of bottom friction, and u_d, v_d the components of current at some depth d, below the sea surface.

An alternative to (7) which is appropriate in a linear model, is a linear stress condition, namely,

$$F_B=k\rho u_d,\quad G_B=k\rho v_d \tag{8}$$

Rather than using slip conditions at the sea-bed, a no-slip bottom boundary condition can be used, namely,

$$u_h=v_h=0 \tag{9}$$

However in this case, Davies[11] has shown that it is very important to accurately resolve the high shear layer which occurs near the sea-bed, when this condition is used.

2.2. *Transformation to sigma co-ordinates*

In general the depth h varies over a sea region. Therefore if the same number of grid boxes in the vertical, and hence the same vertical resolution, is to be maintained at each horizontal grid point, it is necessary to use sigma co-ordinates.

Transforming equations (1) to (4) from the interval $-\zeta \leqslant z \leqslant h$, into the constant interval $0 \leqslant \sigma \leqslant 1$, can be accomplished using the sigma transformations,

$$\sigma = (z + \zeta)/(h + \zeta) \tag{10}$$

Using (10), equations (1) to (4) in sigma co-ordinates become,

$$\frac{\partial \zeta}{\partial t} + \frac{\partial}{\partial x}\left[(h+\zeta)\int_0^1 u \, d\sigma\right] + \frac{\partial}{\partial y}\left[(h+\zeta)\int_0^1 v \, d\sigma\right] = 0 \tag{11}$$

$$\frac{\partial u}{\partial t} + u\frac{\partial u}{\partial x} + v\frac{\partial u}{\partial y} + w^*\frac{\partial u}{\partial \sigma} - \gamma v = -g\frac{\partial \zeta}{\partial x} + \left(\frac{1}{h+\zeta}\right)^2 \frac{\partial}{\partial \sigma}\left(N\frac{\partial u}{\partial \sigma}\right) \tag{12}$$

$$\frac{\partial v}{\partial t} + u\frac{\partial v}{\partial x} + v\frac{\partial v}{\partial y} + w^*\frac{\partial v}{\partial \sigma} + \gamma u = -g\frac{\partial \zeta}{\partial y} + \left(\frac{1}{h+\zeta}\right)^2 \frac{\partial}{\partial \sigma}\left(N\frac{\partial v}{\partial \sigma}\right) \tag{13}$$

where

$$w^* = \frac{1}{h+\zeta}\left\{\frac{\partial \zeta}{\partial t}(1-\sigma)\right\} + \frac{1}{h+\zeta}\frac{\partial}{\partial x}\left\{(h+\zeta)\int_\sigma^1 u \, d\sigma\right\} + \frac{1}{h+\zeta}\frac{\partial}{\partial y}\left\{(h+\zeta)\int_\sigma^1 v \, d\sigma\right\} \tag{14}$$

Similarly transforming surface and sea-bed boundary conditions (5) and (6) to sigma co-ordinates, gives, at the sea surface,

$$-\rho\left(N\frac{\partial u}{\partial \sigma}\right)_0 = (h+\zeta)F_s, \quad -\rho\left(N\frac{\partial v}{\partial \sigma}\right)_0 = (h+\zeta)G_s \tag{15}$$

and at the sea-bed,

$$-\rho\left(N\frac{\partial u}{\partial \sigma}\right)_1 = (h+\zeta)F_B, \quad -\rho\left(N\frac{\partial v}{\partial \sigma}\right)_1 = (h+\zeta)G_B \tag{16}$$

where in these equations u, v, w^* are the components of velocity in sigma co-ordinates.

3. SOLUTION USING A THREE DIMENSIONAL FINITE DIFFERENCE GRID

3.1. *Finite difference grid*

In this section the finite difference form of equations (11) to (14) is developed using finite difference grids in both the horizontal and vertical space domains.

In the horizontal a staggered grid is used, in which ζ and w are computed at the same grid point, denoted by a $\bigcirc$ in Figure 1, with u evaluated at $+$ points and v evaluated at $\times$ points (see Figure 1). Grid lines are parallel and have a grid spacing of Δx and Δy respectively in the x and y directions (Figure 1).

A staggered finite difference grid is also employed in the vertical, with horizontal velocity points situated at the centres of grid box sides (see Figure 2(a)), and vertical velocity and viscosity points at the centre of upper and lower faces (Figure 2(a)). The sea surface elevation point is situated in the centre of the upper face of the top grid box.

In order to increase resolution in the sea surface and sea bed boundary layers (see Figure 2(a), (b)) a mesh of varying thickness $\Delta\sigma_k$ (where k refers to the kth grid box from the sea surface) can be used in the vertical.

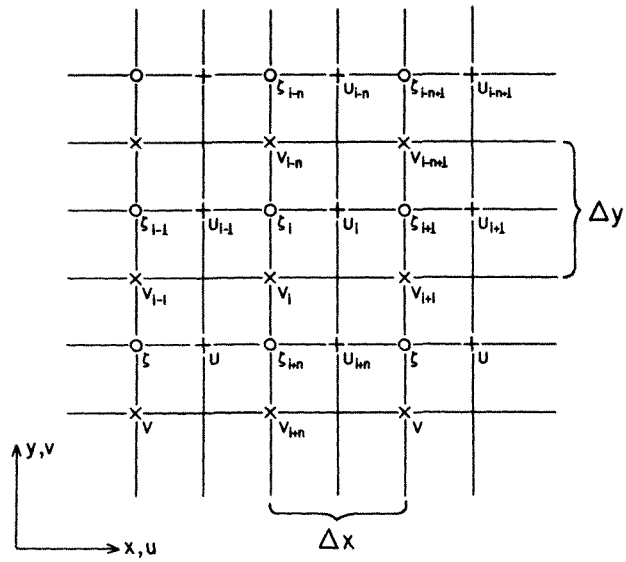

Figure 1. Horizontal finite difference grid in the x, y plane (○ denotes a ζ point, + a u-point, × a v-point)

The region from sea surface to sea-bed, is divided into m boxes of thickness $\Delta\sigma_k$, through the vertical (Figure 2(b)). The notation used for velocity components on this grid is of the form, $u_{i,k}$, $v_{i,k}$, $w_{i,k}$, with i denoting the horizontal grid point (Figure 1) and k the vertical grid box (Figure 2(b)). Since elevation is only specified on the upper face of the top grid box (Figure 2(a)), elevation points are denoted by ζ_i, where i is the horizontal grid point. If eddy viscosity is taken as constant in the horizontal, although varying through the vertical, then N_k denotes the eddy viscosity at level k (Figure 2(b)). In a practical computation, N would be related to the current velocity (see, for example, Reference 12); in this case N would vary in the horizontal. This variation has been included in the algorithms developed here, but for ease of presentation the horizontal variation of N is not included in the development described here.

Centred finite differences are used to represent spatial derivatives both in the horizontal and the vertical. In order to satisfy surface and sea-bed boundary conditions (15) and (16) when centred finite differences are used in the vertical, with the vertical grid shown in Figure 2(b), it is necessary to introduce fictitious current points $u_{i,0}$, $v_{i,0}$ a distance $\Delta\sigma_1/2$ above the sea surface, and $u_{i,m+1}$, $v_{i,m+1}$ a distance $\Delta\sigma_m/2$ below the sea-bed (see Figure 2(b)).

3.2. *Finite difference form of the boundary conditions*

Using fictitious current points, $u_{i,0}$, $v_{i,0}$ and $u_{i,m+1}$, $v_{i,m+1}$, surface and bottom boundary conditions, in finite difference form at horizontal grid point i are given by,

$$-\rho N_1 \frac{(u_{i,1}-u_{i,0})}{\Delta\sigma_1} = d_i F_s, \qquad -\rho N_1 \frac{(v_{i,1}-v_{i,0})}{\Delta\sigma_1} = e_i G_s \tag{17a}$$

and

$$-\rho N_{m+1} \frac{(u_{i,m+1}-u_{i,m})}{\Delta\sigma_m} = d_i F_B, \quad -\rho N_{m+1} \frac{(v_{i,m+1}-v_{i,m})}{\Delta\sigma_m} = e_i G_B \tag{17b}$$

where $d_i = 0{\cdot}5(h_i + \zeta_i + h_{i+1} + \zeta_{i+1})$ and $e_i = 0{\cdot}5(h_i + \zeta_i + h_{i+n} + \zeta_{i+n})$.

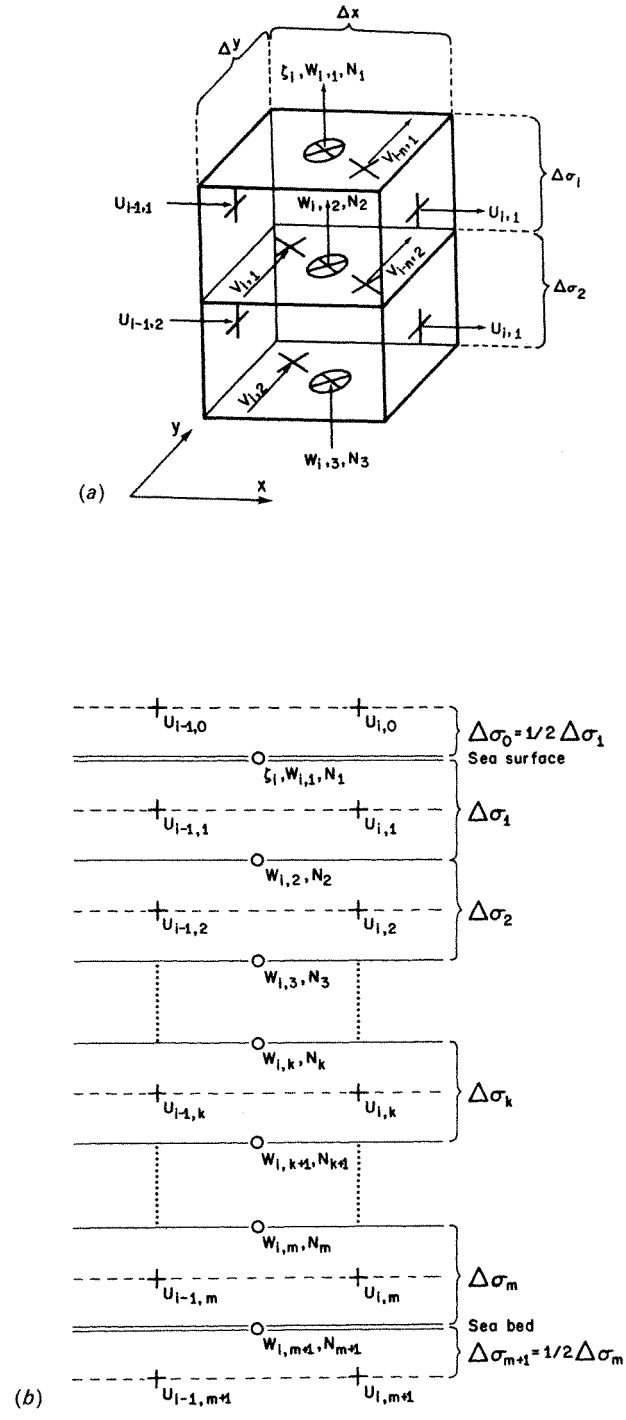

Figure 2. (a) Three-dimensional representation of relative position of grid points. (b) Location of variables in $x - z$ plane

Relating bottom stress linearly to the currents $u_{i,m}$, $v_{i,m}$ at level m, gives for F_B, G_B at grid point i,

$$F_B = k\rho u_{i,m}, \quad G_B = k\rho v_{i,m} \tag{18a}$$

Relating bottom stress linearly to the current at the sea-bed, $z = h$, gives,

$$F_B = k\rho \frac{(u_{i,m} + u_{i,m+1})}{2}, \quad G_B = k\rho \frac{(v_{i,m} + v_{i,m+1})}{2} \tag{18b}$$

If the eddy viscosity at the sea bed can be accurately determined, for example from the bed roughness length[11] and its near bed vertical variation is known, then it is reasonable to use a no-slip condition (equation (9)).

An approximate form of the no-slip bottom boundary condition, (equation (9)) in finite difference form, is given by

$$\left(\frac{u_{i,m} + u_{i,m+1}}{2}\right) = 0, \quad \left(\frac{v_{i,m} + v_{i,m+1}}{2}\right) = 0 \tag{19}$$

3.3. *Calculation of sea surface and sea-bed currents*

It is evident from Figure 2(b), that u and v grid points do not coincide with the sea surface or the sea-bed. However sea surface and sea-bed currents can still be obtained from the model.

Davies and Stephens[13] used two methods to compute surface currents. In the first, the surface current $q_e(u_e$ or $v_e)$ is linearly extrapolated from interior points, using

$$q_e = q_1 - \Delta\sigma_1 \left(\frac{q_2 - q_1}{\Delta\sigma_1 + \Delta\sigma_2}\right) \tag{20}$$

where $q_k(u_k$ or $v_k)$ is the current at level k.

In the second method a linear average with the fictitious point above the sea surface was used, of the form

$$q_a = \tfrac{1}{2}(q_0 + q_1)$$

Using the sea surface boundary condition to eliminate the velocity q_0 at the fictitious point gives,

$$q_a = \frac{1}{2}\left[2q_1 + \frac{\Delta\sigma_1}{\rho N_1}(h + \zeta)Q_s\right] \tag{21}$$

In these equations q_e is the u or v component of surface current computed using linear extrapolation, and q_a is that computed with linear averaging. The term Q_s denotes surface stresses F_s or G_s.

3.4. *Time splitting of the equations of motion*

It is evident from (12) and (13) that at each time step, the majority of the computational time is involved in evaluating the advective terms which occur in these equations. When an explicit time integration method is used to solve these equations, then the size of the time step is limited by the speed of propagation of the gravity wave (the CFL condition). However the advective terms, since they do not involve the gravity waves, can be integrated with a longer time step. By applying a splitting technique the advective terms can be integrated with a longer time step Δt than the linear terms, which are evaluated in a series of shorter time steps τ.

Considering the u equation of motion for illustrative purposes. Writing equation (12) as two separate equations, the first containing the gravity waves and the second the advective terms, gives

$$\frac{\partial u_g}{\partial t} - \gamma v = -g\frac{\partial \zeta}{\partial x} + \frac{1}{(h+\zeta)^2}\frac{\partial}{\partial \sigma}\left(N\frac{\partial u}{\partial \sigma}\right) \tag{22}$$

$$\frac{\partial u_A}{\partial t} = -u\frac{\partial u}{\partial x} - v\frac{\partial u}{\partial y} - w^*\frac{\partial u}{\partial \sigma} \tag{23}$$

where

$$u = u_g + u_A \tag{24}$$

The v equations of motion, equations (13) can be written in a similar manner.

In order to integrate the full equation (12), through a time step Δt, it is necessary because of the C.F.L. constraint to integrate (22) through a number of shorter time steps τ, where $\Delta t = n\tau$.

It is also advantageous to split equation (22) further, into a part describing the mean flow (the external mode) and a part describing the deviations from the mean flow (the internal mode).

Thus, expressing u and v as,

$$u = \bar{u} + u', \quad v = \bar{v} + v' \tag{25}$$

with $\bar{u}, \bar{v}$ denoting components of the depth mean flow, we can obtain from (22) the set of equations

$$\frac{\partial \bar{u}_g}{\partial t} = \gamma \bar{v} - g\frac{\partial \zeta}{\partial x} - \frac{F_B}{\rho(h+\zeta)} + \frac{F_s}{\rho(h+\zeta)} \tag{26}$$

and

$$\frac{\partial u'_g}{\partial t} = \gamma v' + \frac{1}{(h+\zeta)^2}\frac{\partial}{\partial \sigma}\left(N\frac{\partial u}{\partial \sigma}\right) + \frac{F_B}{\rho(h+\zeta)} - \frac{F_s}{\rho(h+\zeta)} \tag{27}$$

By inspection it is evident that adding (26) and (27) we obtain the original equation (22). It is also evident that (26) can be obtained by vertically integrating equation (22) and incorporating sea surface and sea-bed stresses F_s, F_B, since

$$\bar{u} = \frac{1}{h+\zeta}\int_h^{-\zeta} u\,dz, \quad \bar{v} = \frac{1}{h+\zeta}\int_h^{-\zeta} v\,dz \tag{28}$$

The importance of this separation into external and internal parts, lies in the fact that equation (27) does not contain the free surface term $g\partial\zeta/\partial x$ (the gravity wave term). Therefore if an explicit time integration method is used to integrate (26) and (27) through time, then only the time step in (26) is governed by the C.F.L. condition. The time step in (27) does depend however upon stability conditions involving the vertical eddy viscosity.

Thus, if we consider the model problem,

$$\frac{\partial u}{\partial t} = \alpha\frac{\partial^2 u}{\partial \sigma^2} \tag{29}$$

with α a constant, then using an explicit forward time stepping method of the form,

$$\frac{u_k^{t+\Delta t} - u_k^t}{\Delta t} = \alpha\left(\frac{u_{k+1}^t - 2u_k^t + u_{k-1}^t}{(\Delta\sigma_j)^2}\right) \tag{30}$$

where k denotes the k'th grid point, and $k+1$, $k-1$ are grid points on either side, then it can be

readily shown[5,6] that (30) is stable only if

$$\frac{\alpha\Delta t}{(\Delta\sigma_k)^2} \leqslant \frac{1}{2} \tag{31}$$

For the case when,

$$\alpha = N/h^2 \tag{32}$$

condition (32) becomes

$$\Delta t \leqslant \frac{1}{2}\frac{(\Delta\sigma h)^2}{N} \tag{33}$$

Consequently as the vertical grid is refined, i.e. $\Delta\sigma$ decreases, or a solution is required in a shallow region (small h) with a high level of turbulence (high N) then Δt must be reduced. In many oceanographic problems this can lead to a time step which is smaller than that required by the C.F.L. condition. This problem can be avoided by using either an implicit treatment of the term involving the vertical eddy viscosity or by using the DuFort–Frankel method[3] or that developed by Saul'ev.[4]

In the DuFort–Frankel method, three time levels are used, and unconditional stability is obtained by centring the diffusion term in time. For example applying the DuFort–Frankel method to equation (29), gives

$$\frac{u_k^{t+\Delta t} - u_k^{t-\Delta t}}{2\Delta t} = \frac{\alpha}{(\Delta\sigma_k)^2}(u_{k+1}^t - u_k^{t+\Delta t} - u_k^{t-\Delta t} + u_{k-1}^t) \tag{34}$$

In the case of the Saul'ev method, only two time levels are used, but an alternating direction sweep method is employed at alternate time steps. For example, applying it to (29) gives.

Upsweep (sweep direction from k low to k high),

$$\frac{u_k^{t+\Delta t} - u_k^t}{\Delta t} = \frac{\alpha}{(\Delta\sigma_k)^2}(u_{k+1}^t - u_k^t - u_k^{t+\Delta t} + u_{k-1}^{t+\Delta t}) \tag{35}$$

Downsweep (sweep direction from k high to k low),

$$\frac{u_k^{t+\Delta t} - u_k^t}{\Delta t} = \frac{\alpha}{(\Delta\sigma_k)^2}(u_{k+1}^{t+\Delta t} - u_k^{t+\Delta t} - u_k^t + u_{k-1}^t) \tag{36}$$

By this means an explicit time integration method is obtained (Details of the method are well known and the interested reader is referred to Reference 5 for a full description of its implementation).

3.5. *Finite difference form of the hydrodynamic equations*

Considering the continuity equation (11), using centred differencing in space, (see Figures 1 and 3) at grid point i, we obtain

$$\frac{\partial\zeta_i}{\partial t} = \frac{-1}{\Delta x}\left\{d_i \sum_{k=1}^{m} u_{i,k}\Delta\sigma_k - d_{i-1}\sum_{k=1}^{m} u_{i-1,k}\Delta\sigma_k\right\}$$
$$-\frac{1}{\Delta y}\left\{e_{i-n}\sum_{k=1}^{m} v_{i-n,k}\Delta\sigma_k - e_i\sum_{k=1}^{m} v_{i,k}\Delta\sigma_k\right\} \tag{37}$$

where d_i, e_i are as defined before, $\Delta\sigma_k$ denotes vertical grid spacing (see Figure 2(b)).

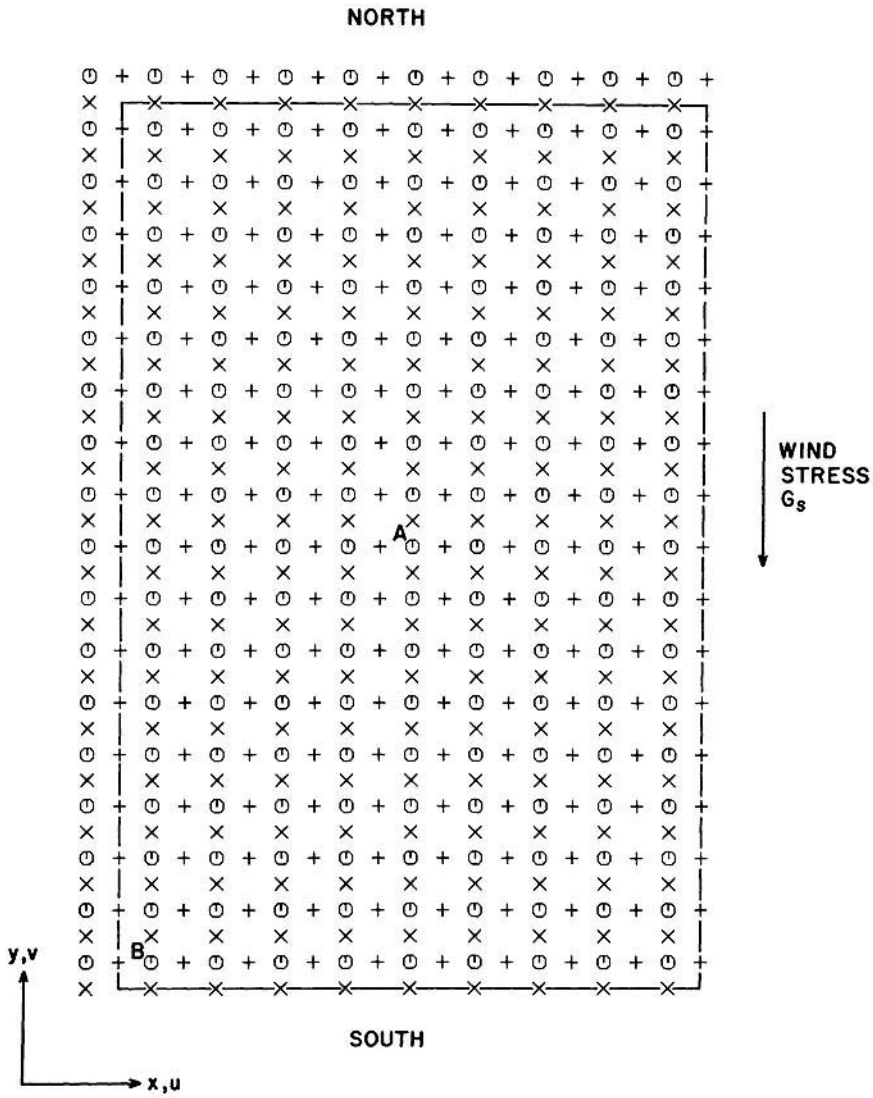

Figure 3. Finite difference grid over the rectangular basin, ○ a ζ-point, + a U-point, × a v-point —land boundary.

In general the grid spacing in the vertical can be varied, to give enhanced resolution in the boundary layers. A number of finite difference representations are possible with such a grid, and the effect of varying grid resolution and difference scheme upon numerical accuracy is discussed in detail by Roache.[6]

For the u equation of motion, without time splitting, equation (12) at point $u_{i,k}$ gives

$$\frac{\partial u_{i,k}}{\partial t} = \gamma \tilde{v}_{i,k} - g\left(\frac{\zeta_{i+1} - \zeta_i}{\Delta x}\right) + \frac{1}{d_i^2}\frac{1}{\Delta\sigma_k}\left\{\frac{N_{k+1}(u_{i,k+1} - u_{i,k})}{0{\cdot}5(\Delta\sigma_{k+1} + \Delta\sigma_k)} - \frac{N_k(u_{i,k} - u_{i,k+1})}{0{\cdot}5(\Delta\sigma_k + \Delta\sigma_{k-1})}\right\} - S_{uk} \tag{38}$$

Similarly for the v equation of motion (13) we obtain,

$$\frac{\partial v_{i,k}}{\partial t} = -\gamma \tilde{u}_{i,k} - g\left(\frac{\zeta_i - \zeta_{i+n}}{\Delta y}\right) + \frac{1}{e_i^2}\frac{1}{\Delta\sigma_k}\left\{N_{k+1}\frac{(v_{i,k+1} - v_{i,k})}{0{\cdot}5(\Delta\sigma_{k+1} + \Delta\sigma_k)} - \frac{N_k(v_{i,k} - v_{i,k-1})}{0{\cdot}5(\Delta\sigma_k + \Delta\sigma_{k-1})}\right\} - S_{vk} \tag{39}$$

where

$$\tilde{u}_{i,k} = 0{\cdot}25(u_{i,k} + u_{i-1,k} + u_{i-1+n,k} + u_{i+n,k}) \tag{40}$$

$$\tilde{v}_{i,k} = 0{\cdot}25(v_{i,k} + v_{i+1,k} + v_{i+1-n,k} + v_{i-n,k}) \tag{41}$$

In these equations S_{uk} and S_{vk} are the finite difference forms of the advective terms as given by Davies and Stephens[13] and will not be repeated here.

We next consider briefly the time differencing of equations (37), (38) and (39).

3.5.1. DuFort–Frankel method. The DuFort–Frankel method involves three time levels and has been applied previously[1,2] to the solution of the hydrodynamic equations without splitting of internal and external flows. However both Sengupta *et al.*[1] and Stephens[2] found that the length of the time step for which stable solutions could be computed was determined by the viscosity term.

Since three time levels are involved in the DuFort–Frankel method there is the possibility of even time step and odd time step (see Figure 4) solutions diverging.[6] However this can be prevented by periodically averaging the solutions computed from even and odd time steps. Stephens[2] time averaged his solution every five time steps in order to retain stability. This time averaging did however significantly damp the solution.[2] These numerical difficulties of the DuFort–Frankel method are considered in detail later in this section.

We now consider the various time levels at which the right hand sides of (37), (38) and (39) can be evaluated, while still retaining a forward time stepping integration method. In order to clearly illustrate the time stepping method, the horizontal differencing terms in (37), (38) and (39) will not be repeated in full but rather are represented by functions f, f_1, f_2 of ζ, u and v.

Applying the DuFort–Frankel method to equation (37) with the right hand side evaluated at the lower time step, gives

$$\frac{\zeta^{t+\Delta t} - \zeta^{t-\Delta t}}{2\Delta t} = f(u^{t-\Delta t}, v^{t-\Delta t}) \tag{42}$$

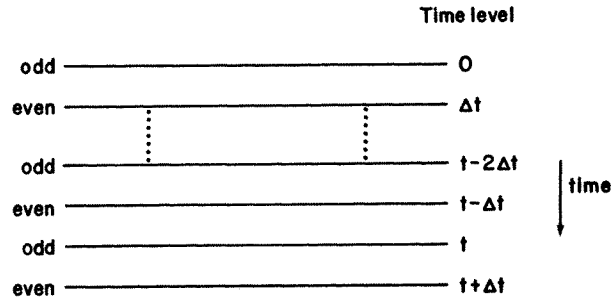

Figure 4. Schematic representation of the finite difference grid in time used with the DuFort–Frankel scheme. Time levels are designated alternately odd and even

Alternatively with the right hand side of (37) at the central time step gives

$$\frac{\zeta^{t+\Delta t}-\zeta^{t-\Delta t}}{2\Delta t}=f(u^t,v^t) \tag{43}$$

Similarly applying the DuFort–Frankel method to the linear u-equation (27) omitting the g subscript for convenience with the advective term separated off by time splitting, gives

$$\frac{u_k^{t+\Delta t}-u_k^{t-\Delta t}}{2\Delta t}=\gamma v^t-f_1(\zeta^{t-\Delta t})-f_2(u_{k+1}^t,u_k^{t+\Delta t},u_k^{t-\Delta t},u_{k-1}^t) \tag{44}$$

Alternatively centering the elevation gradient terms gives

$$\frac{u_k^{t+\Delta t}-u_k^{t-\Delta t}}{2\Delta t}=\gamma v^t-f_1(\zeta^t)-f_2(u_{k+1}^t,u_k^{t+\Delta t},u_k^{t-\Delta t},u_{k-1}^t) \tag{45}$$

and with ζ at the higher time step, we obtain

$$\frac{u_k^{t+\Delta t}-u_k^{t-\Delta t}}{2\Delta t}=\gamma v^t-f_1(\zeta^{t+\Delta t})-f_2(u_{k+1}^t,u_k^{t+\Delta t},u_k^{t-\Delta t},u_{k-1}^t) \tag{46}$$

A similar set of equations can be drived from the v equation of motion. Equation (46) involves ζ at the higher time step $t+\Delta t$, therefore if an explicit method is used, the continuity equation must be evaluated before the equations of motion. This order of evaluation is used throughout.

In equations (42) and (43) $f(u^t,v^t)$ represents the right hand side of (37) with u and v evaluated at the appropriate time. In (44), (45) and (46), $f_1(\zeta^t)$ represents the gradient term with ζ evaluated at the appropriate time t, and $f_2(u_{k+1}^t,u_k^{t+\Delta t},u_k^{t-\Delta t},u_{k-1}^t)$ represents the DuFort–Frankel time centering of the viscosity term in the same form as that shown in equation (34).

Although u in equations (44), (45) and (46) appears at the higher time levels, it is possible to rearrange the equations so that the finite difference forms of these equations can be integrated forward through time in an explicit manner.

3.5.2. Saul'ev[4] method. An alternative to using a three time level DuFort–Frankel scheme is to use the Saul'ev[4] method. This approach only uses two time levels in the equation of motion; however it does involve a sweep method through the vertical. The direction of this sweep has to be alternated every time step in order to avoid any bias in the method.[5]

When the Saul'ev method is used to represent the diffusion term, then forward time stepping is employed to integrate (37) forward in time, thus,

$$\frac{\zeta^{t+\Delta t}-\zeta^t}{\Delta t}=f(u^t,v^t) \tag{47}$$

Applying the Saul'ev method to the linear u-equation of motion, gives,

Upsweep (sweep in direction of increasing k, i.e. from sea surface to sea-bed)

$$\frac{u_k^{t+\Delta t}-u_k^t}{\Delta t}=\gamma\tilde{v}_k^t-f_1(\zeta^{t+\Delta t})-f_2(u_{k+1}^t,u_k^t,u_k^{t+\Delta t},u_{k-1}^{t+\Delta t}) \tag{48}$$

Downsweep (sweep in direction of decreasing k, i.e. from sea-bed to sea surface),

$$\frac{u_k^{t+\Delta t}-u_k^t}{\Delta t}=\gamma\tilde{u}_k^t-f_1(\zeta^{t+\Delta t})-f_2(u_{k+1}^{t+\Delta t},u_k^{t+\Delta t},u_k^t,u_{k-1}^t) \tag{49}$$

Similar finite difference equations can be developed for the v equation of motion.

In equation (47) $f(u^t, v^t)$ represents the right hand side of (37) with u and v evaluated at time t. In (48) and (49) $f_1(\zeta^{t+\Delta t})$ represents the gradient term with ζ evaluated at $t + \Delta t$. The other possibility is to evaluate ζ at time t. In these equations f_2 represents the Saul'ev differencing of the viscosity term in the form shown in equations (35) and (36).

4. TEST CALCULATIONS WITHOUT TIME SPLITTING

In order to compare the accuracies of the DuFort–Frankel method and that due to Saul'ev; the wind induced circulation in a rectangular closed basin has been calculated. The rectangular basin (Figure 3) has dimensions and rotation representative of the North Sea. The water was initially at rest, and motion in the basin was generated by a uniform northerly wind stress of 15 dyn/cm^2. Parameters used in the calculation were $\Delta x = 400/9$ km; $\Delta y = 800/17$ km; $h = 65$ m; $\gamma = 0{\cdot}44h^{-1}$, $\rho = 1{\cdot}025$ g/cm^3; $g = 981$ cm^2/s; $F_s = 0$ and $G_s = -15$ dyn/cm^2.

With this particular grid spacing, using the C.F.L. condition, $\Delta t < \Delta s/\sqrt{(2gh)}$ with Δs the grid spacing, gives a maximum $\Delta t = 1245$ s (approx. 20 min).

If an explicit method is used for the eddy viscosity term, then with $N = 650$ cm^2/s, and $h = 65$ m, then equation (33) with $\Delta\sigma = 1/m$, gives for the maximum time step, for a range of m,

$m = 5$,	$\Delta t = 1300$	s	(approx. 21 min)
$m = 10$,	$\Delta t = 325$	s	(approx. 5 min)
$m = 15$,	$\Delta t = 144{\cdot}4$	s	(approx. 2·4 min)
$m = 25$,	$\Delta t = 52$	s	(approx. 0·87 min)

A rectangular North Sea basin having the above dimensions was chosen because an accurate solution of this problem (using linear equations, with $N = 650$ cm^2/s) has been computed by a number of authors[13–15] using different numerical methods.

In order to compare the present series of calculations with those computed previously, a linear model was used. The advective terms S_{uk} and S_{vk} were omitted and $h + \zeta$ was replaced by h in the continuity equation and in the equation of motion. A linear law of bottom friction was employed in which bottom stress was related to the current at the sea-bed, using equation (8) with $k = 0{\cdot}2$ cm/s.[14]

4.1. Linear model, with DuFort–Frankel method

In an initial series of calculations with the linear model, the DuFort–Frankel method was used without time splitting of internal and mean flows. In the first series of calculations (calculations a(i), a(ii) and a(iii) see Table I), the right hand side of the continuity equation was evaluated at time t (see equations (37) and (43)) and the various time differencing options given in equations (44) to (46) were employed in the equations of motion. In a second series of calculations (calculations a(iv), a(v) and a(vi), see Table I), the right hand side of the continuity equation was evaluated at time $t - \Delta t$, together with the various time differencing options given in equations (44) to (46). These various options are summarized in Table I.

Initially, a time step of 180 s was used, to be consistent with other numerical calculations[14,15] although subsequently a time step of 540 s was considered. These values were significantly below the C.F.L. condition (i.e. 1245 s).

A range of vertical resolutions, namely $m = 5$, 10, 15 was examined. The effect of time averaging even and odd time step solutions after a number of time steps Δt upon the solution was considered by comparing calculations with no time averaging, with those of time averaging every $40\Delta t$, $5\Delta t$ and $2\Delta t$.

Table I. Summary of various time level options used in the DuFort–Frankel method, without time splitting

Calculation	Right hand side of the continuity equation evaluated at time	Gradient term in equations of motion evaluated at time
a(i)	t	$t-\Delta t$
a(ii)	t	t
a(iii)	t	$t+\Delta t$
a(iv)	$t-\Delta t$	$t-\Delta t$
a(v)	$t-\Delta t$	t
a(vi)	$t-\Delta t$	$t+\Delta t$

In all cases shown in Table I the solutions became unstable before having been integrated for 150 h, with the exception of calculations a(ii) and a(vi) which were stable for $m = 5$ or 10 with $\Delta t = 180$ s provided some time averaging was performed. In the case of $m = 10$, time averaging every $2\Delta t$ was required.

These calculations showed that the DuFort–Frankel method without time splitting was basically unstable. A stable solution could be obtained provided m and Δt were small (i.e. $m = 5$, $\Delta t = 180$ s) and time averaging was employed. However the effect of time averaging was to artificially dampen the solution, with damping increasing the more frequently time averaging was applied. Also the time level at which the various terms were evaluated influenced the damping of the solution. Calculations showed that sea surface elevation at point B (see Figure 3) was significantly influenced by changing the time level at which the various terms were computed. For example values of ζ at point B at time $t = 30$ h in calculation a(iii) were lower than in calculation a(ii), which were also slightly lower than in calculation a(vi).

The reason for this change in ζ between calculation a(iii), a(ii) and a(vi) can be understood from equations (42) to (46); thus, neglecting for illustrative purposes rotation, internal friction and external friction, then using (43) and (45) gives, for

Case a(ii)

$$u^{t+\Delta t} = u^{t-\Delta t} + 2\Delta t f_1(\zeta^{t-2\Delta t} + 2\Delta t f(u^{t-\Delta t}, v^{t-\Delta t})) \tag{50}$$

Case a(iii), using (43) and (46)

$$u^{t+\Delta t} = u^{t-\Delta t} + 2\Delta t f_1(\zeta^{t-\Delta t} + 2\Delta t f(u^t, v^t)) \tag{51}$$

Case a(vi), using (42) and (46)

$$u^{t+\Delta t} = u^{t-\Delta t} + 2\Delta t f_1(\zeta^{t-\Delta t} + 2\Delta t f(u^{t-\Delta t}, v^{t-\Delta t})) \tag{52}$$

Representing diagramatically time integration with the DuFort–Frankel method as a series of odd and even time levels (Figure 4) it is evident from equation (50) that in case a(ii), $u^{t+\Delta t}$ (an even time level) depends upon the current $u^{t-\Delta t}$ at other even time levels; the coupling of the odd time levels coming through $\zeta^{t-2\Delta t}$ (an odd time level). In case a(iii) however, equation (51) shows that $u^{t+\Delta t}$ (even) again depends upon $u^{t-\Delta t}$ (even), but is coupled to u^t (odd) through the elevation gradient term, which involve u^t, v^t through continuity. The arrangement of the time differencing in case a(vi) (equation (52)), however is such that $u^{t+\Delta t}$ (even) depends entirely upon ζ and u at other even time steps and without Coriolis or friction would not be coupled to the odd time steps.

Since coupling together of odd and even solutions by time averaging them introduces damping

into the solution, with more damping the more frequently they are coupled, then in an analogous manner, case a(iii) (equation (51)) with its coupling through the elevation gradient term of the odd and even levels, will be significantly more heavily damped than case a(ii) in which coupling only occurs through $\zeta^{t-2\Delta t}$, and the least damped will be case a(vi) where without the frictional and Coriolis terms no coupling occurs. It is evident from the calculations that this conclusion is found in practice.

4.2. *Linear model, with Saul'ev method*

In order to compare the accuracy of the Saul'ev and DuFort–Frankel methods, the previous calculation of wind induced motion in a rectangle was repeated but the Saul'ev differencing method was used for the viscosity term. A forward time stepping method was employed and the right hand side of the continuity equation was evaluated at time t. In an initial series of calculations the term $g\partial\zeta/\partial x$ was evaluated at time $t+\Delta t$, and in a subsequent series at time t.

Calculation b(i). Gradient term at $(t+\Delta t)$; equations (47), (48) and (45). Initially N was set at 650 cm^2/s and a range of time steps Δt from 180 s, 540 s to 900 s was employed, with $m = 5$, 15, 25 grid boxes in the vertical. Bottom stress was computed in terms of current at the bottom level.

Table II shows sea surface u and v components of current (calculated using (20) and (21)) computed using five and twenty-five grid boxes in the vertical, with time steps of 180 s, 540 s and 900 s at point A in the centre of the basin (Figure 3). It is evident from this Table that with a time step of 180 s, no numerical instabilities occurred even with $m = 25$. However when the time step was increased to 900 s the calculation with $m = 25$ exhibited some physically unrealistic time step oscillation in u, v and ζ. In theory the Saul'ev method should be unconditionally stable, however it is evident that in the solution of the three dimensional equations this is not so. A time step of 900 s is below the C.F.L. condition of 1245 s for this problem and also the calculation with $m = 5$ was stable

Table II. Sea surface elevations at point B (Figure 3) and surface current at point A, at time $t = 8{\cdot}6$ h and 150 h computed using the Saul'ev method for a range of time steps $\Delta t = 180$ s, 540 s, 900 s, with $m = 5$ and 25

Time step Δt			$m=5$ Time (h) 8·6	$m=5$ Time (h) 150·0	$m=25$ Time (h) 8·6	$m=25$ Time (h) 150·0
180 s	Sea surface current (cm/s)	u_a	−12·81	−11·93	−15·04	−13·18
		u_e	−16·34	−15·23	−15·24	−13·37
		v_a	−49·20	−36·98	−48·86	−35·65
		v_e	−44·10	−31·77	−48·65	−35·44
	Elevation (cm)	ζ	172·3	103·1	171·6	102·1
540 s	Sea surface current (cm/s)	u_a	−13·31	−11·92	−16·56	−13·53
		u_e	−16·82	−15·22	−16·77	−13·73
		v_a	−49·40	−37·00	−50·86	−35·95
		v_e	−44·30	−31·79	−50·65	−35·73
	Elevation (cm)	ζ	171·8	103·1	166·9	101·0
900 s	Sea surface current (cm/s)	u_a	−13·56	−11·91	−15·37	−11·49
		u_e	−17·07	−15·21	−15·59	−11·69
		v_a	−49·86	−37·06	−51·59	−35·00
		v_e	−44·74	−31·85	−51·38	−34·79
	Elevation (cm)	ζ	171·2	103·0	160·4	110·2

with a 900 s time step. The problem of poor numerical accuracy when $m = 25$ and $\Delta t = 900$ s is considered later in detail in connection with the DuFort–Frankel method.

The effect upon the accuracy of the solution of using a 900 s time step can be seen in Table II, solution with $m = 5$, by comparing currents 8·6 h after the onset of the wind field (the time when ζ at point B is a maximum) computed using a 180 s and a 900 s time step. It is evident from the Table that there are some significant differences of the order of 0·8 cm/s in the surface current.

After 150 h the difference between currents computed with 180 s and 900 s time steps is less than 0·1 cm/s. This is because at 150 h a near steady state has been reached and consequently errors in time discretization are no longer important.

It is also interesting to compare the differences between sea surface currents computed by averaging (u_a, v_a) (see equation (21)) and by extrapolation (u_e, v_e) (see equation (20)). It is apparent from Table II, that the differences between averaged and extrapolated currents diminishes as the number of grid boxes m increases. This is to be expected since in the limit as m goes to infinity the two values will coincide. Since both averaged and extrapolated currents can be easily computed, the differences between them can be used as a guide to the accuracy of the solution. From Table II it is apparent that solutions computed with $m = 25$, should be accurate in this case to the order of 0·2 cm/s, whereas solutions computed with $m = 5$ would have a lower accuracy of order 3 cm/s. This point is also considered later in connection with Table V.

Calculation b(ii). Gradient term at time t; equations (47), (48) and (49). When the Saul'ev method was used to integrate the hydrodynamic equations with the gradient terms $\partial\zeta/\partial x$, $\partial\zeta/\partial y$ in the equations of motion evaluated at time t, it was not possible to obtain a stable solution for any of the cases considered previously. It is therefore particularly important to evaluate the continuity equation before the equations of motion and hence to use this computed ζ at the higher time level in the equations of motion. Hence the order of calculation is:

(1) calculation of $\zeta(t + \Delta t)$ from u^t, v^t using the continuity equation
(2) evaluation of $u(t + \Delta t)$, $v(t + \Delta t)$ from the equations of motion (2) and (3) using the Saul'ev method with the terms $\partial\zeta/\partial x$ and $\partial\zeta/\partial y$ evaluated using $\zeta(t + \Delta t)$.

5. TEST CALCULATIONS WITH TIME SPLITTING OF INTERNAL AND EXTERNAL MOTION

In the previous section both the DuFort–Frankel and the Saul'ev methods were applied to the solution of the linear hydrodynamic equations, without time splitting of internal and external motions. In this section we consider the application of both methods again to the linear equations, but now external motions and internal motions have been separated in the equations of motion, for example equations (26) and (27).

5.1. Linear equations with the DuFort–Frankel method

The continuity equation, and the two equations of motion describing the mean flow (the external mode) are integrated using a forward time stepping method, with a time step τ. The equations describing the internal flow (equation (27) and its v equivalent) are integrated using the DuFort–Frankel method with a time step Δt.

In order to examine the accuracy of the solution using a range of time steps τ and Δt, and to test if the DuFort–Frankel method remains stable when external and internal motions are treated separately (equations (26), (27)) the previous calculations were repeated, using the time split

algorithm. A number of calculations were performed with a range of $\tau = \Delta t$ time step, namely 180 s, 540 s, 900 s and two m values of 5 and 25 were used. Hence although a splitting of internal and external motions was applied, the same time step was used in each i.e. $\tau = \Delta t$.

Computed sea surface currents in the centre of the basin, point A in Figure 3 for a range of time steps $\Delta t = \tau = 180$ s, 540 s, 900 s, with five and twenty-five grid boxes, are given in Table III. Sea surface elevation at Point B (see Figure 3) is also given.

Values of elevation and surface current computed with an external time step $\tau = 180$ s and internal time steps Δt of 540 s and 900 s, using the DuFort–Frankel method with time splitting are given in Table IV. In all cases the solution remained stable.

Table III. Sea surface elevations at point B (Figure 3) and surface currents at point A, at time $t = 8{\cdot}6$ h and 150 h computed using the time-split DuFort–Frankel method for a range of time steps $\Delta t = \tau = 180$ s, 540 s, 900 s with $m = 5$ and 25

Time step			$m = 5$ Time (h)		$m = 25$ Time (h)	
180 s	Sea surface current (cm/s)	u_a	−12·56	−11·93	−13·63	−13·19
		u_e	−16·09	−15·23	−13·84	−13·39
		v_a	−49·15	−36·97	−47·85	−35·63
		v_e	−44·06	−31·76	−47·63	−35·41
	Elevation (cm)	ζ	172·8	103·1	173·7	102·1
540 s	Sea surface current (cm/s)	u_a	−12·45	−11·93	−11·17	−13·21
		u_e	−15·97	−15·23	−11·38	−13·40
		v_a	−49·17	−36·97	−44·56	−35·59
		v_e	−44·08	−31·76	−44·35	−35·37
	Elevation (cm)	ζ	173·4	103·0	176·3	102·1
900 s	Sea surface current (cm/s)	u_a	−12·05	−11·93	−26·66	−13·18
		u_e	−15·55	−15·23	−26·97	−13·38
		v_a	−49·35	−36·97	−44·94	−35·56
		v_e	−44·25	−31·76	−44·71	−35·34
	Elevation (cm)	ζ	173·8	103·0	184·2	101·9

Table IV. Sea surface elevations at point B (Figure 3) and currents at point A, at $t = 8{\cdot}6$ h and 150 h computed using the time-split DuFort–Frankel method with an external time step $\tau = 180$ s, and internal time steps $\Delta t = 540$ s and 900 s

Time step			$m = 5$ Time (h) 8·6	150·0	$m = 25$ Time (h) 8·6	150·0
$\tau = 180$ s $\Delta t = 540$ s	Sea surface current (cm/s)	u_a	−12·50	−11·93	−11·23	−13·22
		u_e	−16·02	−15·23	−11·43	−13·41
		v_a	−49·15	−36·97	−44·58	−35·59
		v_e	−44·06	−31·76	−44·35	−35·37
	Elevation (cm)	ζ	172·9	103·1	175·7	102·2
$\tau = 180$ s $\Delta t = 900$ s	Sea surface current (cm/s)	u_a	−12·12	−11·93	−26·53	−13·18
		u_e	−15·62	−15·23	−26·84	−13·38
		v_a	−49·24	−36·97	−45·02	−35·56
		v_e	−44·15	−31·76	−44·79	−35·34
	Elevation (cm)	ζ	172·8	103·1	183·5	102·1

It is apparent from Tables III and IV, that by separating the internal and external motions it is possible to obtain a stable solution using the DuFort–Frankel method. The solution appears stable even when $m = 25$ and a time step $\Delta t = 900$ s is employed (see Table III). However it is evident that in this case the computed currents (in particular the u component) at $t = 8{\cdot}6$ h are significantly greater than those computed with $\Delta t = 540$ s or 180 s. In the case in which $m = 5$, however, there is little difference in velocities computed with $\Delta t = 180$ s or 900 s. This suggests that time discretization errors, although greater when $\Delta t = 900$ s compared with 180 s are not responsible for the difference in accuracy which occurs when $m = 25$.

In order to understand why there is a significant difference in currents computed using $\Delta t = 180$ s and 900 s with $m = 25$ at $t = 8{\cdot}6$ h but not when $m = 5$, it is necessary to consider the physics of wind induced flow. In the problem considered here motion is induced in a sea area at rest by the sudden application of a high surface wind stress. When a forward time stepping algorithm is used with the vertical grid spacing shown in Figure 2(b) it is evident that within the first time step a non-zero current can only be generated at the uppermost grid box in Figure 2(b). With the difference scheme used here this non-zero value propagates through the vertical at one grid point per time step. Consequently it takes $2m$ time steps for this initial disturbance to propagate from sea surface to sea-bed and back to the sea surface. In order for the solution to be independent of this initial 'shock like' condition a couple of propagations from sea surface to sea-bed of the disturbance would probably be required and this would take $4m$ time steps. For $m = 5$, it would therefore require 20 time steps to remove the initial conditions. With a time step as large as 900 s, and $m = 5$, only a period of 900×20 s $= 5$ h would be required to remove the influence of the initial conditions and consequently in this case solution at $t = 8{\cdot}6$ h in Tables III and IV would be independent of the initial condition. It is evident from these tables that there are only slight differences between solutions computed with $m = 5$ and $\Delta t = 180$ s or 900 s.

Considering now the case when $m = 25$, which would require $4m = 100$ time steps to remove the effect of the initial conditions. When $\Delta t = 180$ s, this requires a period of 5 hours, however when $\Delta t = 900$ s, a period of 25 h is required. Consequently when $m = 25$, the velocity at time $t = 8{\cdot}6$ h is still influenced by initial conditions, explaining the differences found in Tables III and IV. However after 150 h the various solutions given in Tables III and IV are not significantly different.

As a further check on the accuracy of the computed currents when a range of internal time steps was used, namely $\Delta t = 180$ s, 540 s, 900 s, with the external time step $\tau = 180$ s and $m = 25$, currents at $t = 30$ hours were compared (Table V) with published values[15] computed using a functional

Table V. Comparison of surface and bottom currents 30 h after the onset of the wind field computed using 25 grids in the vertical with an external time step of 180 s and a range of internal time steps $\Delta t = 180$ s, 540 s, 900 s. Also shown are values computed by Davies and Owen[15] using functions in the vertical

		Internal time step			Galerkin method[15]	
		$\Delta t = 180$ s	$\Delta t = 540$ s	$\Delta t = 900$ s	Ten Legendre polynomials	Ten Chebyshev polynomials
Sea surface current (cm/s)	u_a	−15·01	−16·48	−18·33	−15·12	−15·06
	u_e	−15·22	−16·68	−18·56		
	v_a	−33·25	−33·53	−35·75	−33·20	−33·20
	v_e	−33·03	−33·.32	−35·55		
Sea-bed current (cm/s)	u_a	6·75	6·53	9·38	7·03	6·96
	u_e	6·83	6·61	9·54		
	v_a	11·78	11·86	11·82	11·75	12·07
	v_e	11·87	11·95	11·80		

representation in the vertical and a time step of 180 s. At a time $t = 30$ h, even with a time step of 900 s, the effect of the initial conditions has been nearly removed and it is evident from Table V that computed currents obtained either by averaging or extrapolation when $m = 25$ are in good agreement with the accurate solution of Davies and Owen[15] computed with a time step of 180 s.

This series of calculations has shown that by writing the hydrodynamic equations in the form of equations describing external and internal motion, a stable solution using the DuFort–Frankel method can be obtained, with a time step as large as 900 s and with vertical grid resolution as high as 25 vertical grid levels. This is to be compared with a time step of 52 s which would be required if a forward time stepping method was used to integrate the viscous term. However it is evident that in a wind induced flow problem in which motion is created from rest by a suddenly applied wind stress, it is important to use a sufficiently small time step, particularly with a high vertical grid resolution, if the effects of this initial shock are not to corrupt the solution.

5.2. *Linear equations with the Saul'ev method*

As we have shown a stable solution of the hydrodynamic equations could be obtained using the Saul'ev method without separating internal and external motion. However such a separation is obviously advantageous in deep water or with fine horizontal grids where the C.F.L. condition imposes a small time step. By performing this separation the internal flow field can be integrated using the Saul'ev method with a significantly longer time step than that used for the external flow.

The implementation of the Saul'ev method with this time splitting is the same as for the DuFort–Frankel method. The test calculations described previously yielded similar results to those computed with the DuFort–Frankel method except for the case when the time step was 900 s. In this case spurious physically unrealistic oscillations appeared in the solution of a similar nature to those computed without separation of internal and external flows. For this reason the DuFort–Frankel method was applied to the solution of the non-linear equations described in the next section. Also the DuFort–Frankel method has second order accuracy in time compared with the first order accuracy of the Saul'ev method,[5] and for this reason it is preferable to use it when the internal time step is long.

5.3. *Solution of the non-linear hydrodynamic equations*

As a further check on the accuracy and stability of the DuFort–Frankel method when the non-linear terms are present the previous calculation was repeated using the full non-linear equations (1), (2) and (3). An accurate solution of this problem with which comparisons can be made is given in Reference 16.

The time splitting method described previously in which the external flow was computed with a different time step from the internal flow and the advective terms was used. The same time step was used for the internal flow as for the advective terms. Following Davies,[16] the linear time step τ and the non-linear time step Δt were taken as $\tau = 180$ s, $\Delta t = 4\tau = 720$ s.

Calculations were performed using five and twenty-five grid boxes in the vertical. Surface, mid-depth and sea-bed currents computed with $m = 25$, agreed to within 2 cm/s (an acceptable error) of the accurate solution published by Davies.[16]

6. CONCLUDING REMARKS

Stability analysis of the one dimensional diffusion problem[5] has shown that both the DuFort–Frankel and Saul'ev methods are unconditionally stable in this case. However in this paper we

have shown that when the DuFort–Frankel method is applied to the discretization of the vertical diffusion of momentum term in the three dimensional hydrodynamic equations it is no longer unconditionally stable. This point has been noted by a number of authors[1,2] who found it necessary because of this problem to use a small time step[2] to retain numerical stability.

In this paper we have shown that the term involving the gradient of sea surface elevation within the equations of motion is responsible for the instability of the DuFort–Frankel method when applied to the discretization of the vertical viscosity term. However when the Saul'ev method is used calculations show that it remains stable.

Stable solutions using the DuFort–Frankel method have however been obtained by splitting the hydrodynamic equations into a set describing the mean flow and a set describing deviations from the mean flow. This latter set contain the vertical viscous term but not the term involving the gradient of sea surface elevation.

Once the hydrodynamic equations are separated in this manner it is computationally efficient to integrate them using different time steps. This would be particularly economic in a model of a deep estuary when a fine grid was used in the horizontal. In such a situation the C.F.L. condition would require the use of a small time step for the mean flow, although the internal flow could be integrated with a much longer time step.

Calculations are presently in progress using the time-split DuFort–Frankel method developed here in more physically realistic situations and results will be reported subsequently.

ACKNOWLEDGEMENTS

I am indebted to Dr. N. S. Heaps and Dr. C. V. Stephens for a number of useful discussions during the course of this work.

The care taken by Mr. R. Smith in preparing the diagrams and Mrs. P. Lynch in typing the paper is appreciated.

REFERENCES

1. S. Sengupta, H. P. Miller and S. Samuel, 'Effect of open boundary condition on numerical simulation of three-dimensional hydrothermal behaviour of Biscyne Bay, Florida', *Int. j. numer. methods fluids*, **1**, 145–169 (1981).
2. C. V. Stephens, 'Hydrodynamic modelling developments for the west coast of the *British* Isles', *Ph.D. Thesis*, Liverpool University, 1983.
3. E. C. DuFort and S. P. Frankel, 'Stability conditions in the numerical treatment of parabolic differential equations', *Math. Tables and Other Aids to Computation*, **7**, 135–152 (1953).
4. V. K. Saul'ev, 'On a method of numerical integration of the equation of diffusion', *Doklady Akad. Nauk USSR*, **115**, 1077 (1957).
5. R. D. Richtmyer and K. W. Morton, *Difference methods for Initial-value Problems*, 2nd edn, Interscience Publishers, 1967.
6. J. P. Roache, *Computational Fluid Dynamics*, Hermosa Publishers, Alburquerque New Mexico, 1972.
7. A. M. Davies, 'Formulating a three-dimensional hydrodynamic sea, model using a mixed Galerkin-finite difference method', K. P. Holz *et al.* (eds) *Finite Elements in Water Resources, Proceedings of the 4th International Conference on Finite Elements in Water Resources*, Springer-Verlag, 1982, pp. 5–27–5–41.
8. B. Johns, P. C. Sinha, S. K. Dude, U. C. Mohanty and A. D. Rao, 'Simulation of storm surges using a three-dimensional numerical model an application to the 1977 Andhra cyclone', *Quart J. R. Met. Soc.*, **109**, 211–224 (1983).
9. N. A. Phillips, 'A coordinate system having some special advantages for numerical forecasting', *J. Meteorol*, **14**, 184–186 (1957).
10. N. G. Freeman, A. M. Hale, and M. B. Danard, 'A modified sigma equation approach to the numerical modelling of great lakes hydrodynamics', *J. Geophys. Research*, **77**, 1050–1060 (1972).
11. A. M. Davies, 'Formulation of a linear three-dimensional hydrodynamic sea model using a Galerkin-eigenfunction method', *Int. j. numer. methods fluids*, **3**, 33–60 (1983).
12. A. M. Davies and G. K. Furnes, 'Observed and computed M_2 tidal currents in the North Sea', *Journal of Physical Oceanography*, **10**, 237–257 (1980).
13. A. M. Davies and C. V. Stephens, 'Comparison of the finite difference and Galerkin methods as applied to the solution of the hydrodynamic equations', *Applied Mathematical Modelling*, **7**, 226–240 (1983).

14. N. S. Heaps, 'On the numerical solution of the three-dimensional hydrodynamic equations for tides and storm surges', *Mem. Soc. r. Sci. Liege Ser 6*, **2**, 143–180 (1972).
15. A. M. Davies and A. Owen, 'Three-dimensional numerical sea model using the Galerkin method with a polynomial basis set', *Applied Mathematical Modelling*, **3**, 421–428 (1979).
16. A. M. Davies, 'Application of the Galerkin method to the formulation of a three-dimensional non-linear hydrodynamic sea model', *Applied Mathematical Modelling*, **4**, 245–256 (1980).